Supporting Information

Spontaneous migration of cellular aggregates: from giant keratocytes to running spheroids

Grégory Beaune,[a,b,1] Carles Blanch-Mercader,[a,b,c,1] Stéphane Douezan,[a,b] Julien Dumond,[a,b] David Gonzalez-Rodriguez,[a,b,d] Damien Cuvelier,[a,b,e,f] Thierry Ondarçuhu,[g] Pierre Sens,[a,b] Sylvie Dufour,[e,h] Michael P. Murrell,[i,j] and Françoise Brochard-Wyart[a,b,2]

[a]*Sorbonne-Université Paris 05, UMR 168, Institut Curie, 26 rue d'Ulm, 75248 Paris Cedex 05, France*

[b]*CNRS, UMR, UMR 168, Institut Curie, 26 rue d'Ulm, 75248 Paris Cedex 05, France*

[c]*Departament de Fısica de la Materia Condensada, Universitat de Barcelona, Barcelona 08028, Spain.*

[d]*LCP-A2MC, Institut Jean Barriol, Universite de Lorraine, 1 bd Arago, Metz 57078, France.*

[e]*Sorbonne Université Paris 05, UMR 144, Institut Curie, 26 rue d'Ulm, 75248 Paris Cedex 05, France*

[f]*CNRS, UMR, UMR 144, Institut Curie, 26 rue d'Ulm, 75248 Paris Cedex 05, France*

[g]*Institut de Mécanique des Fluides de Toulouse (IMFT), 4 Université de Toulouse, CNRS, Toulouse, France.*

[h]*INSERM, U955, Equipe 06, Créteil, 94000, France; Université Paris Est, Faculté de Médecine, Créteil, 94000, France.*

[i]*Departments of Physics & Biomedical Engineering, Yale University, 217 Prospect Street, New Haven, CT 06511, USA*

[j]*Systems Biology Institute, Yale University, 840 West Campus Drive, West Haven, CT 06516, USA*

[1]*These authors contributed equally to this work.*

www.pnas.org/cgi/doi/10.1073/pnas.1811348115

[2]*To whom correspondence should be addressed. E-mail: Francoise.Brochard@curie.fr*

A. Materials and Methods

Cell Culture and Aggregates Preparation. We use murine sarcoma Ecad cells expressing E-cadherins at their surface (1). Cells are cultured at 37 °C under 95% air/ 5% CO_2 atmosphere in culture medium consisting of Dulbecco's Modified Eagle Medium (DMEM) enriched with 10% calf serum. Upon reaching confluence, cells are prepared for aggregation following the agitation method (2). Aggregates ranging from 50 to 400 μm in diameter are obtained from 5 mL of cell suspension in CO_2-equilibrated culture medium at a concentration of 4×10^5 cells per mL in 25 mL Erlenmeyer flasks, which are placed on a gyratory orbital shaker at 90 rpm at 37 °C for 30 h. The flasks are pretreated with 2% dimethylchlorosilane in chloroform to prevent adhesion of cells to the glass surface.

Preparation of Coated Glass Substrates. 25 mm circular glass coverslips were sonicated in ethanol for 5 min, dried at room temperature and exposed to deep UV for 5 min. Fibronectin (Sigma-Aldrich) coating was performed using a 0.1 $mg.mL^{-1}$ solution of fibronectin in PBS solution (pH 7.4) for 45 min at RT. Coverslips are then rinsed with PBS (pH 7.4).

Preparation of Polyacrylamide (PAA) Substrates. Flexible PAA gels are created by adapting a published technique (3). The substrate is prepared by allowing PAA solutions to polymerize between two chemically modified glass cover slips (Fisher Scientific, Pittsburgh, PA). A 25 mm-diameter glass coverslip is sonicated in ethanol for 10 min, dried at room temperature and exposed to deep UV for 5 min. 100 μL of 3-APTES (3-aminopropyltriethoxysilane, Sigma-Aldrich, St. Louis, MO) are added onto the surface for 5 min and then 100 μL of distilled water are added for 10 min. The glass cover slip is thoroughly rinsed with ultrapure water to wash away any remaining 3-APTES solution. Then, 100 μL of 0.5%v glutaraldehyde (Sigma-Aldrich) in water is added onto the cover slip for 30 min. The glass cover slip is subsequently rinsed with water. PAA gel solutions are prepared using a 40% w/v acrylamide stock solution (BioRad, CA, USA) and a 2% w/v bisacrylamide

stock solution (BioRad, CA, USA). PAA gel solutions are prepared with acrylamide and bis-acrylamide at final volume concentrations of 10% w/v and between 0.03 and 0.15% w/v respectively for gels with rigidities between 2.8 and 16.7 kPa. To polymerize the solution, 1 µL TEMED (FisherBiotech) and 10 µL of 10% ammonium persulfate are added with the appropriate amount of water to yield a final volume of 1 mL. A fixed volume of 20 µL of the PAA solution is immediately pipetted onto the center of the 25 mm diameter glass coverslip. A second untreated 25 mm-diameter coverslip is then carefully placed on top of the PAA solution. The polymerization is completed in about 30 min and the top cover slip is slowly peeled off and the gels have nearly ideal elastic behavior. A heterobifunctional crosslinker, sulfo-SANPAH (sulfosuccinimidyl6(40-azido-20-nitrophenylamino) hexanoate, Pierce Biotechnology, USA), is used to crosslink fibronectin molecules onto the surface of the gel. 500 µL of an HEPES solution (pH = 8.5) containing sulfo-SANPAH with a mass concentration of 0.2 $mg.mL^{-1}$ and EDC (1-ethyl-3-[3-dimethylaminopropyl]carbodiimide hydrochloride; Sigma-Aldrich) with a mass concentration of 2 $mg.mL^{-1}$ is pipetted onto the gel surface. The PAA gel is then placed 10 cm below an ultraviolet lamp for 10 min. It is then washed with PBS at pH 8.5. After the PBS solution is aspirated, 100 µL of a 0.1 $mg.mL^{-1}$ fibronectin solution is pipetted on top of the PAA gel. After 45 min, the gel is rinsed with PBS at pH 8.5 for 10 min. The cover slip with the attached polyacrylamide gel is placed at the bottom of a chamber for the experiment. The PAA gels fabricated in this manner were determined to be about 40 µm thick just after formation and 80 µm after equilibrium for 2 hours when the cell medium is added.

Aggregate Spreading Experiments and Microscopy. Aggregates were placed on a fibronectin-coated glass or PAA coverslip that forms the bottom of a cylindrical experimental chamber filled with CO_2-equilibrated culture medium maintained at 37 °C using a heating platform. To prevent evaporation, the open surface was sealed with mineral oil.

Brightfield images have been taken using an inverted microscope (Zeiss Axiovert 100) equipped with a ×10 0.45 objective. Videos are recorded with a CCD camera (Photometrics Cascade 512B, Roper Scientific) at an acquisition rate of 1 frame every 5 min.

Images (512 x 510 pixels) were exported from the instrument software in TIFF format and visualized using the ImageJ software package v.1.46r (National Institutes of Health, Bethesda, MD) (4).

Image Analysis. The trajectories of the aggregates were plotted using the Manual Tracking plug-in of ImageJ software. To be more precise the taken values were obtained by tracing the contours of the aggregate, using ImageJ software and taking the center's coordinates of the enclosed area. Data were exported to Microsoft Excel for mathematical and statistical analysis using Chemotaxis and Migration tool v2.0 (5). As mentioned previously, all the experiments have been recorded with an acquisition rate of 1 frame every 5 min. Because aggregates move slowly, measuring manually their position each 5 min may induce some error on the determination of their velocity. We choose to measure their position each 15 min. The different delay times to compute velocities between frames for the different rigidities are indicated in the following table (Table S1).

Table S1. Time of aggregate's motion and delay times between frames chosen to compute velocities of aggregates in function of the rigidity of the gel.

Rigidity of the gel	Times of aggregate's motion to compute velocities	Delay times between frames
16.7 kPa	12 h	15 min
10.6 kPa	12 h	15 min
9 kPa	3 days	15 min

7.6 kPa	3 days	15 min
2.8 kPa	2 days	15 min

Role of the frame rate:

1) Curvilinear velocity

We reanalyzed the data of the figure 2 measuring the location of the aggregate on each frame. It corresponds to a delay time dt of 5 min. Then, we plotted the curvilinear velocity of the aggregate in function of the time for dt = 5 min (in blue), dt = 15 min (in red), and dt = 60 min (in green). The results can be observed on the following figure (Fig. S1).

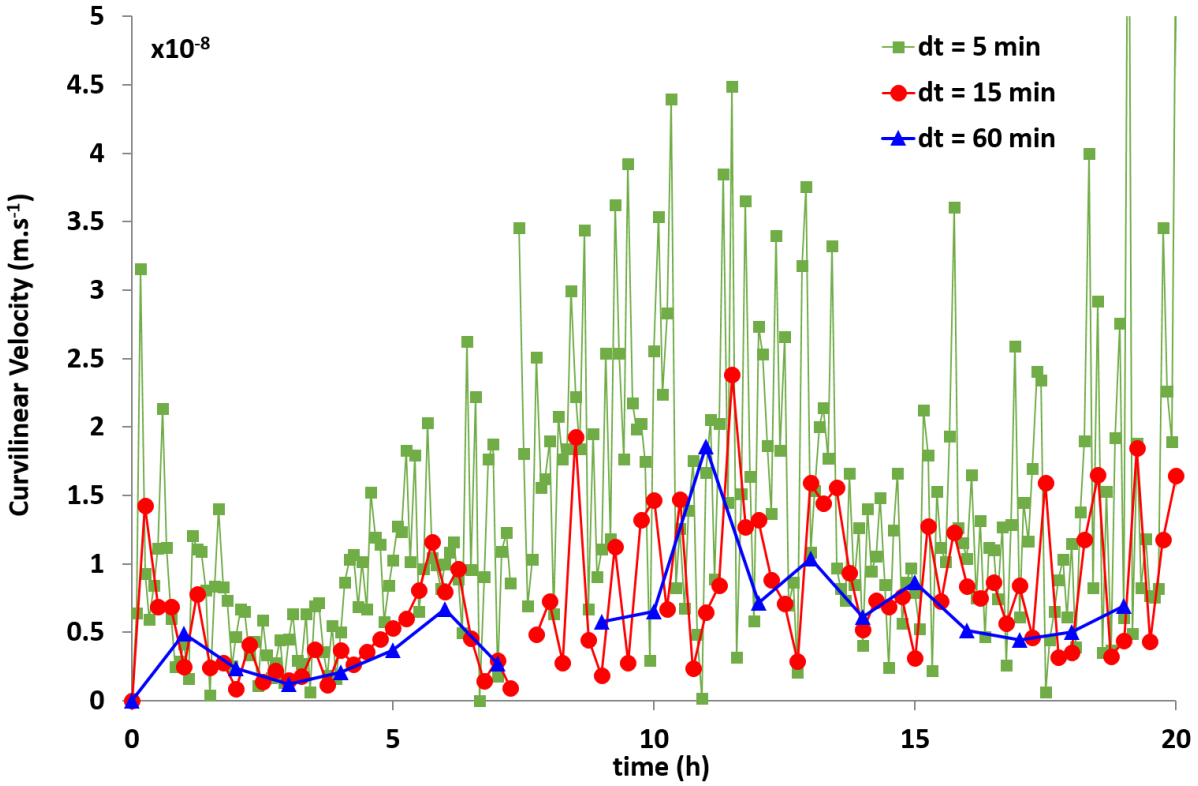

Fig. S1. Curvilinear velocity of an aggregate with the motion of a giant keratocyte in function of delay times between frame (dt) of 5 min, 15 min, and 60 min.

The obtained results in function of dt are indicated in the following table (Table S2).

Table S2. Comparison of the average curvilinear and directionality in function of dt for an aggregate with a giant keratocyte motion.

dt	Average curvilinear velocity	Directionality
5 min	1.7×10^{-2} µm/s	0.4
15 min	0.9×10^{-2} µm/s	0.7
60 min	0.8×10^{-2} µm/s	0.8

These results show that the average curvilinear velocity reaches a plateau for dt =15mn and above. The results reported in the main text correspond to a homogeneous delay times between frames of 15 minutes. Thus the unit times is common and comparisons between different experimental cases are meaningful.

The velocity fields were mapped by PIV analysis. Stacks of images were analyzed by using the MatPIV software package for MATLAB (The MathWorks, Natick, MA) (6) as previously described in *Petitjean et al.*(7). The delay time for all PIV analysis were 5 min.

The Matlab program used to calculate the tangential velocities of the velocity fields has been developed by Michael P. Murrell.

Mean squared displacement (MSD) was used to fit models of stochastic cellular motion. $MSD(t) = [r(t + t_0) - r(t_0)]^2$, where $r(t_0)$ is the initial location of the cell aggregate and $\boldsymbol{r(t+t_0)}$ is the new position after time $\boldsymbol{t}$.

The MSD data was used to determine the migration behaviors of cellular aggregates. MSD is proportional to t^{α}, with α characterizing the motion. α = 1 indicates a random motion and α = 2 indicates a persistent motion. To be more specific, in the case of random walk the MSD should be fitted by $MSD(t) = 4Dt$, where-t is the time, and D is the diffusion coefficient. We tested whether a persistent walk model or a random walk model was appropriate for describing aggregate trajectories. Coordinates were obtained by tracing the contours of aggregates, using ImageJ software and taking the center's coordinates of the enclosed area. MSD is calculated with steps of 15 min.

2) Period of stick-slip

On the figure below (Fig. S2) we focus on the velocity of the aggregate in figure 2D for dt = 15 min. We indicate the correspondence between the peaks and the stick-slip motion on the video S2. They are referenced with the same number. Note that the time on the video does not perfectly match the peaks because the increase of the velocity (slip) happens after the rupture of the film. Rupture locations are indicated with arrows. This figure shows that dt = 15 min reflects well what can be seen on the video and that it is easy to attribute peaks to slick-slip motions, which are clearly distinguished from noise. Indeed, we also highlight with blue circles small peaks in the figure that cannot be observed on the movie and that can be attributed to noise.

Our discussion above on the choice of dt to analyze the curvilinear velocity is also relevant here. Indeed, with dt = 60 min, we only observe 3 peaks and we cannot see the detailed motion of the aggregate. With dt = 5 min, on the other hand, we cannot distinguish the real motion of the aggregate from the noise. This supports our choice of dt = 15 min to analyse the data, as this choice of unit time allows to both resolve aggregate motion and to disciminate real motion from noise.

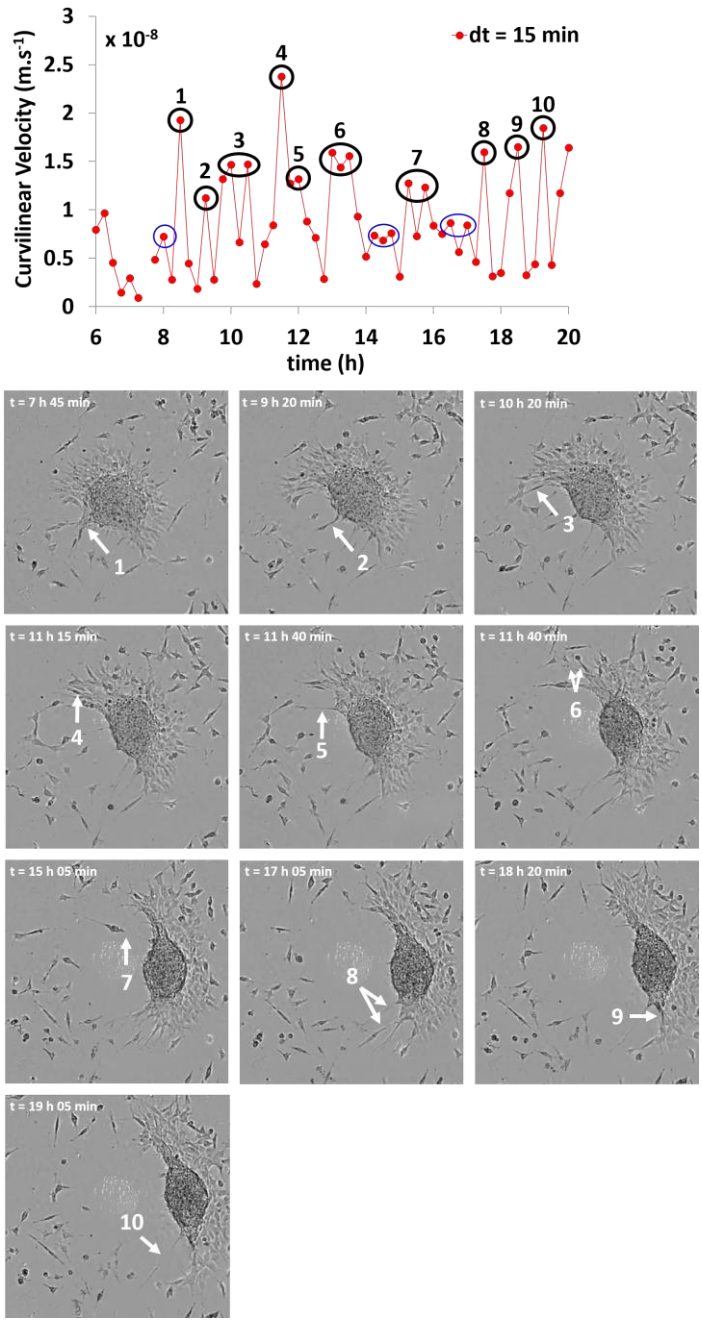

Fig. S2. Correspondence between peak velocities of the aggregate in figure 2D for dt = 15 min and the stick-slip motion on the video. They are referenced with the same number. Rupture locations are indicated with arrows.

Force Measurements. We are using a slightly modified protocol for the preparation of PAA substrates from the one previously described. In this case the fluorescent beads stock solution (*d* = 200 nm, Invitrogen, F8810) is diluted 10 times with the polyacrylamide gel solution. We compare the images of the gel-embedded beads before and after the aggregates have been

deposited on the substrate at different times. We compare these two images to calculate a sub-diffraction-limited displacement of the beads due to traction by the cell aggregate. The Displacement fields are calculated using PIV that runs on Matlab (Mathworks) available at http://www.oceanwave.jp/software/mpiv/.

Running droplets. The running droplets consist of a 0.05 M solution of 1H,1H,2H,2H perfluorodecyltrichlorosilane (96%, Alfa Aesar) in octane (99%, Thermo Fisher Scientific). The glass slides are rinsed in isopropanol and cleaned during 5 minutes by corona treatment using a BD-20 device (ElectroTechnic products) in order to obtain a complete wetting situation. The 5 µL droplets are deposited on the substrate using a micropipette. The droplets motion is recorded with a PCO.1200hs high speed camera (PCO.imaging, Germany) at a rate of 266 fps and an exposure time of 500 µs. The movies are analyzed using the ImageJ software.

B. Figures

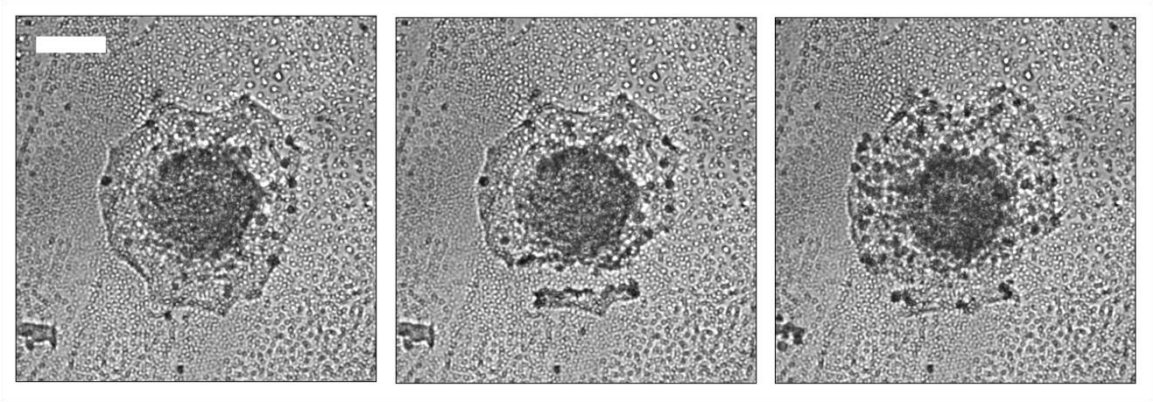

Fig. S3. The precursor film resulting from the spreading of an aggregate on a rigid fibronectin-coated surface (glass substrate, E = 70 GPa) heals when scratched by a needle. Scale bar = 100 µm.

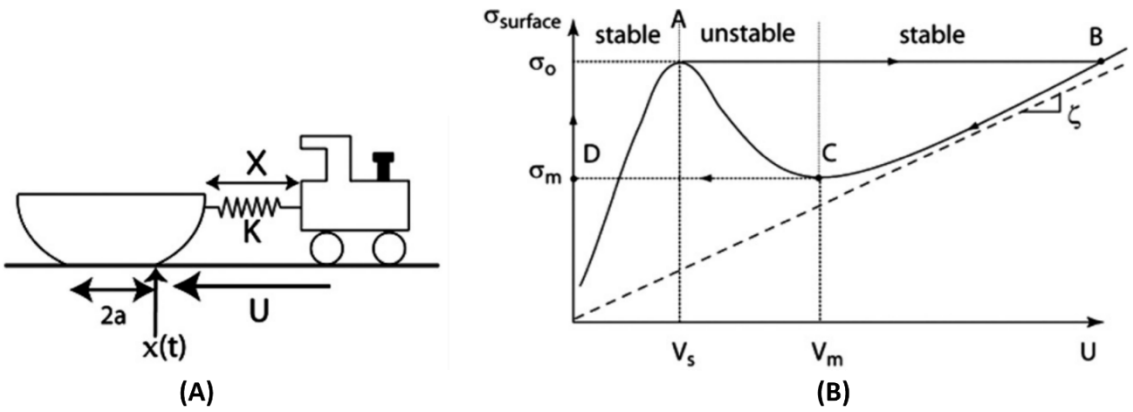

Fig. S4. (A) The aggregate is self-propelled by a small locomotive at a velocity U. The spring constant is K. When the aggregate stick, the force increases up to a maximal force where it slides (B) Stress variations σ (force per unit area) as a function of the sliding velocity U. leading to stick-slip motion (8).

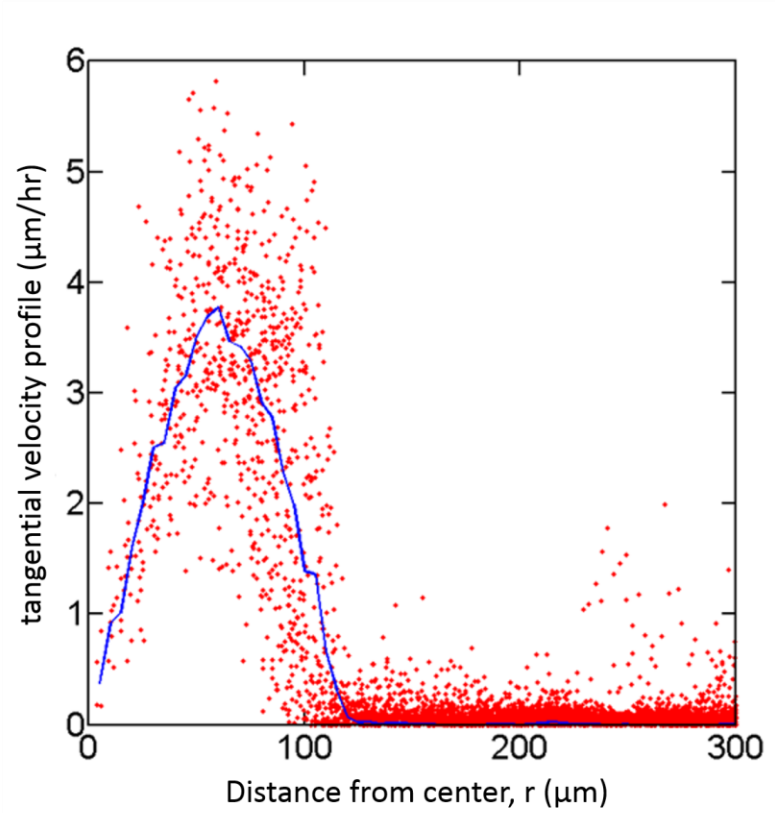

Fig. S5. Tangential velocity of a swinging aggregate in function of the distance from its center, t = 2 h 45 min after it has been deposited on a PAA substrate (E = 10.6 kPa). The radius of the aggregate is of 60 µm and the angular velocity $\Omega = 1 \times 10^{-4}$ rad.s^{-1}.

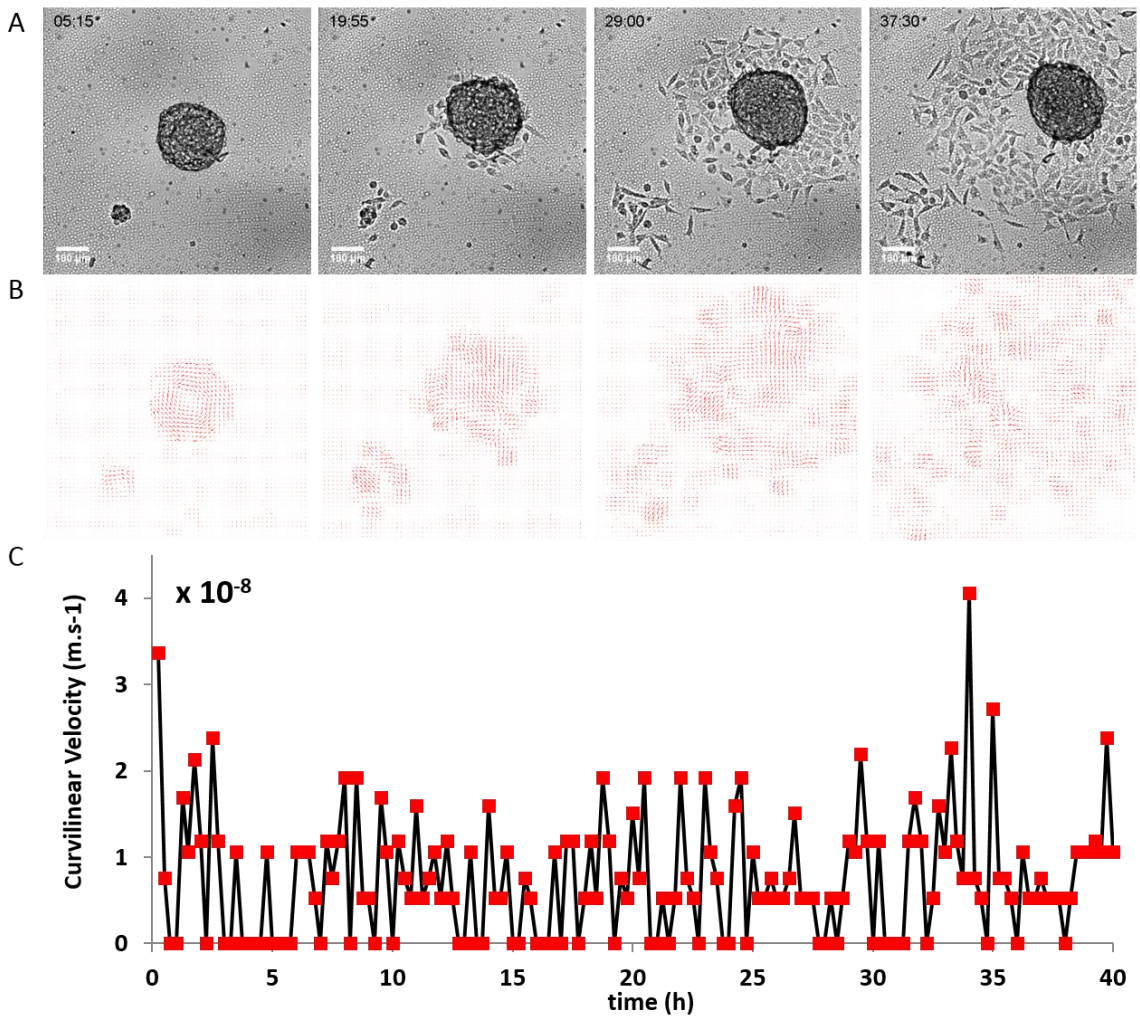

Fig. S6. (A) Spreading film and motility of an aggregate on a PAA gel (E = 7.4 kPa) observed in bright field at different times. (B) Velocity vector fields (PIV) of the aggregate migration from (A). (C) Time evolution of the curvilinear velocity of the aggregate (time step = 15 min).

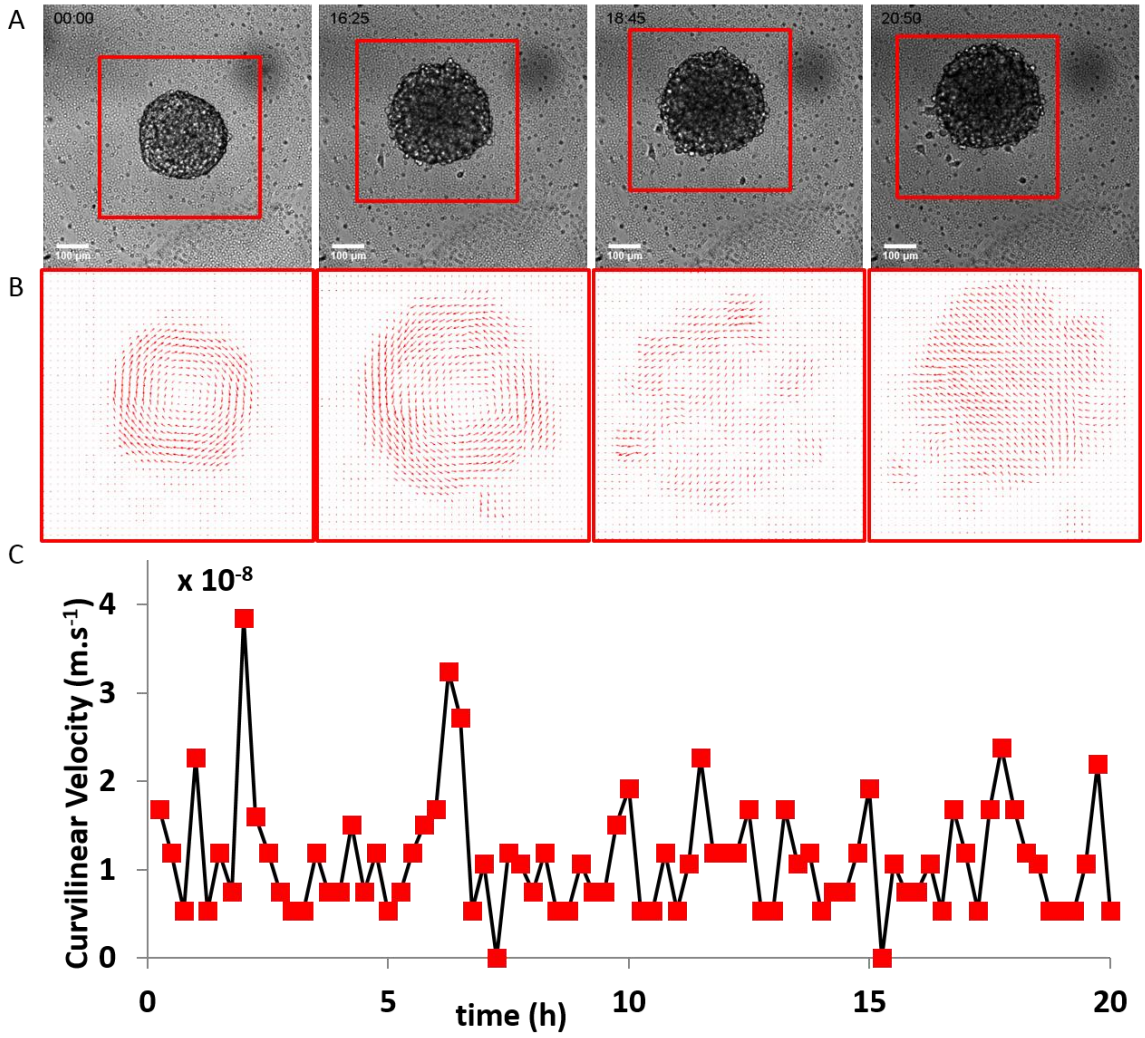

Fig. S7. (A) Spreading film and motility of an aggregate on a PAA gel (E = 2.8 kPa) observed in bright field at different times. (B) Velocity vector fields (PIV) of the aggregate migration from (A). (C) Time evolution of the curvilinear velocity of the aggregate (time step = 15 min).

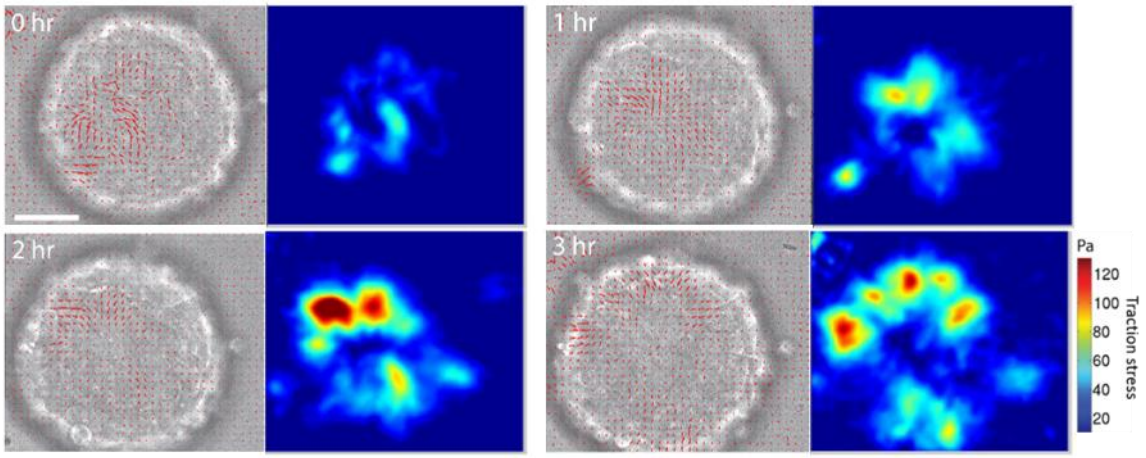

Fig. S8. Bright field images and traction stress applied by an aggregate during the first few hours after it has been deposited on a PAA gel with E = 7.4 kPa. The scale bar corresponds to 100 um.

C. Study of motion of cellular aggregates in chemical gradient and spontaneous motion interpreted in the framework of reactive wetting

Chemotaxis is the phenomenon whereby cells or multicellular organisms direct their movements in response to chemical cues (9). We investigate the chemical sensing of a cellular aggregate to determine if chemotaxis can induce the displacement of an aggregate. Experimentally, we have realized a gel substrate with two adjacent surfaces of different adhesion properties. Half of the substrate is coated with fibronectin (adhesive), and the other half is a raw PAA gel (non adhesive). Cellular aggregates are deposited homogenously on the bivalent surface. Figure S9A shows that the aggregates deposited in the fibronectin-coated region (A, left part) spread as expected (complete wetting regime). Aggregates placed on the raw gel (A, right part) remain spherical (zero-wetting).

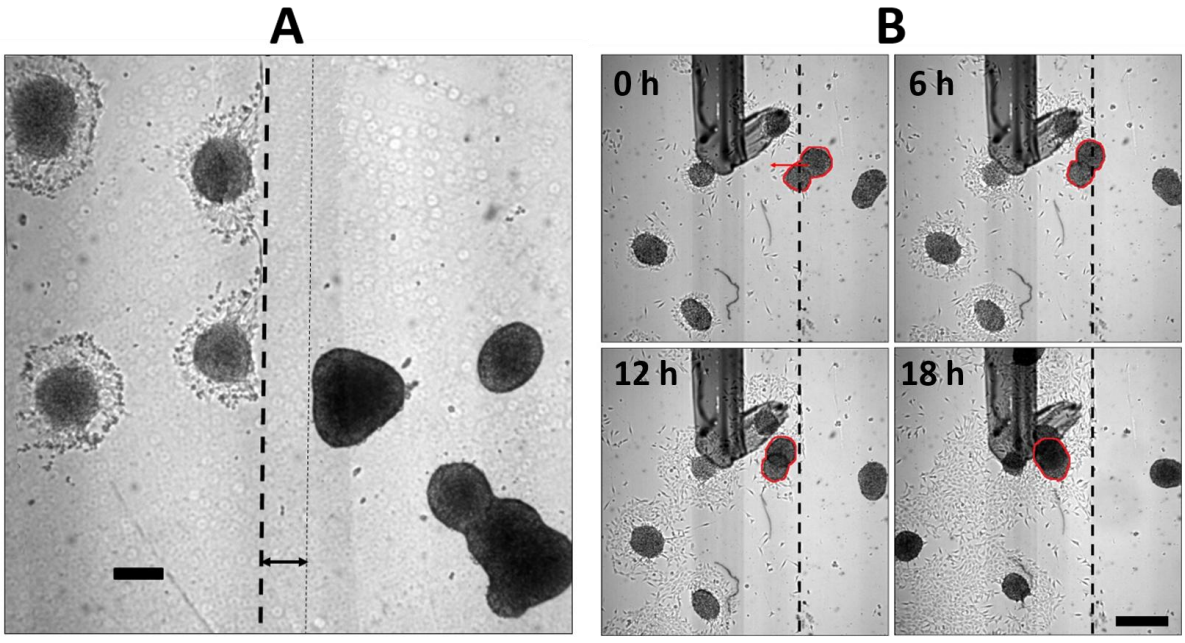

Fig. S9 (A) Final state of spreading of aggregates on an adhesive gradient: Aggregates deposited on the fibronectin-coated patch are in complete wetting regime, whereas the aggregates placed on the raw gel surface remain spherical. Scale bar = 200 µm. (B) An aggregate placed near the boundary crosses the interface to go toward the adhesive patch at a velocity $V \approx 0.5\ \mu\text{m. min}^{-1}$ and finally spreads. Scale bar = 500 μm.

We observe that aggregates placed within a region of width ~100-150 µm move toward the fibronectin-coated area and eventually spread on the adhesive substrate (Fig. S9B). This

motion, due to a gradient of substrate adhesiveness, occurs with an average speed

$U \approx 3\times10^{-3}$ µm.s^{-1}.

An aggregate moving across the boundary experiences an attraction by the chemical favorable ligand equal to the difference between the adhesion energies W_{CF} on the fibronectin substrate (CF = cell-fibronectin) and W_{CG} on the gel substrate (CG = cell-gel). The displacement toward the adhesive surface is analogous to the displacement of a liquid drop on a divalent surface (10). The surfaces seen by both sides of the aggregate are different as illustrated in Figure S10.

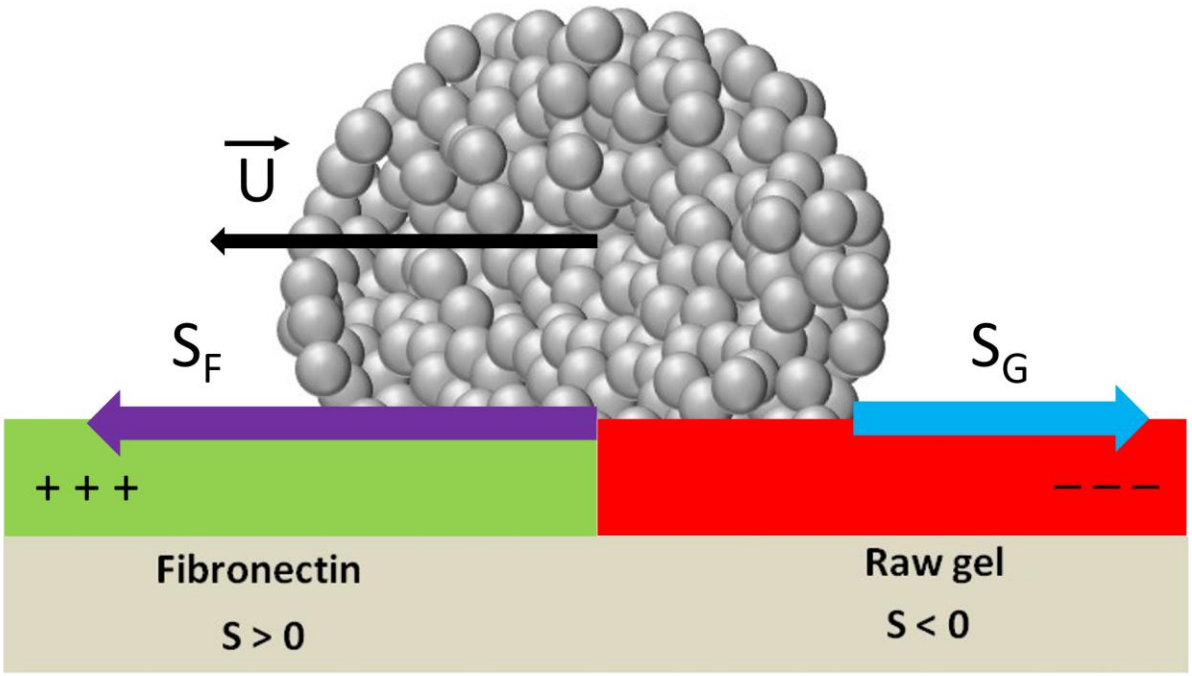

Fig. S10. Schematic representation of an aggregate placed on the boundary between adhesive and non-adhesive surfaces. The capillary forces are asymmetric and cause the aggregate to move toward the adhesive surface (**U**).

The spreading parameter of the side oriented toward the fibronectin-coated substrate is $S_F = W_{CF} - W_{CC}$, where W_{CC} stands for the adhesion energy between cells (CC=cell-cell). Similarly, the spreading parameter of the side oriented toward the raw gel is

$S_G = W_{CG} - W_{CC}$.

The balance between capillary and friction forces given by Eq. (1) leads to

$S_F - S_G = R\ k\ U$

where R is the aggregate radius and k is a friction coefficient. Therefore, this result shows that droplet on divalent surfaces migrate towards the region where the spreading parameter is larger, that is the fibronectin-coated substrate for cell aggregates.

Remark: Slippage versus rolling regime (Fig. S11)

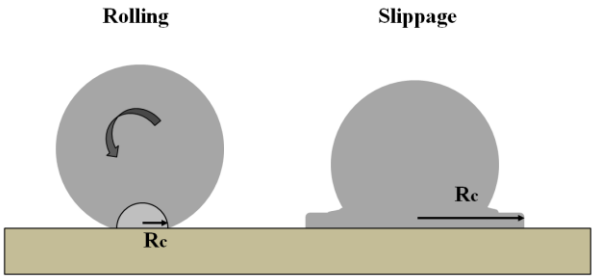

Fig. S11. Schematic representation of the rolling and the slippage of an aggregate placed on the boundary between adhesive and non-adhesive surfaces.

We have assumed that the aggregate slips on the substrate. But the aggregate is viscoelastic and can roll like a spherical jelly particle (running sponge), which has been discussed by P.-G. de Gennes (11). As the aggregate moves at velocity *U*, the dissipation is concentrated near the contact zone, in a region R_c^3 where R_c is the contact radius. The vertical velocity associated with the center of mass velocity is v = U δ/R_c, where δ = R_c^2/R_0. The viscous dissipation can be written

$$T\dot{\Sigma} = \eta \left(\frac{v}{R_c}\right)^2 R_c^3 = \eta \frac{U^2}{R_0^2} R_c^3 \qquad [S3]$$

The energy balance leads to

$$U = \frac{R_0^2}{R_c^2}\left(\frac{S_F - S_G}{\eta}\right) \qquad [S4]$$

Note that $U_{Rolling}/U_{Slippage} = \frac{kR_0^2}{\eta R_c}$. The rolling had been observed for quasi-spherical aggregates, but as the aggregate starts to spread, the radius R_c increases and the rolling is

hindered.

D. Cell polarization-based mechanisms for spontaneous motility of cell aggregates

Here, we detail the theoretical framework used to interpret the collective motion of giant keratocytes in the light of a symmetry-breaking rearrangement of cell polarities. We describe the aggregate-monolayer system as a 1D active incompressible fluid of size R, that we name active droplet. Using a similar physical model for the early dynamics of spreading cell monolayers (12), we denote v(x), p(x) and σ(x) as the velocity, polarity and total stress fields in the x direction. At steady state, we assume that the flux of cells between the aggregate body and the film is negligible, and hence no local cell sources or sinks are accounted for. Taking the cell density constant, the incompressibility condition $\nabla v = 0$ yields v(x)=U. Further, in the lubrication limit, where the thickness of the monolayer e is much smaller than the scale of in-plane variations, the local force balance in the absence of inertial effects,

$$\nabla(\sigma e) = T. \qquad \text{[S5]}$$

This means that the gradients of intercellular stresses σ are balanced by the cell traction stresses on the substrate T (12). The film thickness e is assumed uniform, consistent with spreading of cell monolayers (13). The traction stresses $\mathbf{T} = \mathrm{k}\mathbf{v} - \mathrm{T_o}\mathbf{p}$ are a linear combination of the dissipative friction stresses and the actively-generated traction stresses, where k stands for the friction coefficient and T_0 stands for the amplitude of the active stresses, respectively. In 1D the specific form of the stresses is not necessary to describe the kinetics of the drop. Further, we assume fast relaxational dynamics for the polarity field p that obeys

$$0 = -p + l_c^2 \nabla^2 p \qquad \text{[S6]}$$

where l_c stands for the spatial correlation length of the active traction forces. In the case of expanding monolayers, we choose stress-free boundary conditions, that is the cell forces at

the monolayer interface are balanced by the negligible drag of the extracellular fluid ($\sigma = 0$ at the contact lines), and strong anchoring boundary conditions for the polarity field, that is the polarity p is $-p_r$ and p_a at the receding and advancing front of the active droplet.

In general, the dynamics of active droplets is non-local due to hydrodynamic interactions, and thus non-trivial to predict for arbitrary interfaces. In our 1D description, however, we can derive an exact relation between the slippage velocity of the active droplet U and the cellular forces. Averaging Eq. (S5) over the aggregate length, the left-hand side term vanishes due to stress-free boundary conditions and the right-hand side terms leads to

$$0 = kRU - T_0 R < p > \qquad [S7]$$

where the brackets denote the spatial average over the cell domain. The mean polarity $<p>$ depends on the dissymmetry on cell polarities at the fronts and the ratio between the correlation length l_c and the droplet size R. When $l_c << R$, then $< p > \propto (p_a - p_r) l_c / R$. When $l_c >> R$, then $< p > \propto (p_a - p_r)$. The traction map in Fig. S8 suggests that cell aggregates migrate in the former regime. Notably in the limit, Eq. (S7) can be recast as Eq. (1) by defining the effective spreading parameters $S_a = T_0\, l_c\, p_a$ and $S_r = T_0\, l_c\, p_r$, which only depend on cell material parameters. It is worth noticing that this expression does not depend on the specific form of the stress in 1D. The central result of this appendix is that in order for an aggregate to migrate persistently ($U \neq 0$), traction force on the cell substrate (T_0) as well as a symmetry-breaking rearrangement of cell polarities ($< p > \neq 0$) are demanded at the same time. Therefore, we conclude that the migration direction of active droplets is consistent with the asymmetric cell traction distribution at the monolayer contact line, which is established by a symmetry-breaking dewetting process of the precursor film.

References

1. Chu Y-S, et al. (2006) Prototypical type I E-cadherin and type II cadherin-7 mediate very distinct adhesiveness through their extracellular domains. *J Biol Chem* 281(5):2901–10.
2. Douezan S, et al. (2011) Spreading dynamics and wetting transition of cellular aggregates. *Proc Natl Acad Sci U S A* 108(18):7315–20.
3. Yu-Li W, Pelham Jr. RJ (1998) Preparation of a flexible, porous polyacrylamide substrate for mechanical studies of cultured cells. *Methods Enzymol* 298:489–496.
4. Cordelières F (2004) ImageJ. Available at: http://rsb.info.nih.gov/ij/plugins/track/track.html.
5. Trapp G (2010) Available at http://ibidi.com/software/chemotaxis_and_migration_tool/.
6. Sveen JK (2006) MatPIV. Available at: http://folk.uio.no/jks/matpiv/.
7. Petitjean L, et al. (2010) Velocity fields in a collectively migrating epithelium. *Biophys J* 98(9):1790–800.
8. Wu-Bavouzet F, Clain-Burckbuchler J, Buguin a., De Gennes† P-G, Brochard-Wyart F (2007) Stick-Slip: Wet Versus Dry. *J Adhes* 83(8):761–784.
9. Bagorda A, Parent CA (2008) Eukaryotic chemotaxis at a glance. *J Cell Sci* 121(16):2621–2624.
10. Casagrande C, Fabre P, Raphaël E, Veyssié M (1989) "Janus Beads": Realization and Behaviour at Water/Oil Interfaces. *Europhys Lett* 9(3):251–255.
11. de Gennes P-G (1996) Eponges filantes. *CR Acad Sci Paris* 323(Serie II b):663–667.
12. Blanch-Mercader C, et al. (2017) Effective viscosity and dynamics of spreading epithelia: a solvable model. *Soft Matter* 13(6):1235–1243.

13. Tlili S, et al. (2018) Collective cell migration without proliferation: density determines cell velocity and wave velocity. *R Soc Open Sci* 5(5):172421.

Movies legends

Movie S1. Spreading of a cell aggregate on PAA gel (E = 40 kPa) coated with fibronectin observed in bright field. The spreading of a precursor film around the aggregate is observed. Total movie time: 20 h.

Movie S2. Spontaneous motion of a cell aggregate on a PAA gel (E = 16.7 kPa) observed in bright field. Total movie time: 20 h 30 min.

Movie S3. Motion of a cell aggregate on a PAA gel (E = 10.6 kPa) observed in bright field. Total movie time: 20 h.

Movie S4. Spreading and motion of a cell aggregate on a PAA gel (E = 9 kPa) observed in bright field. Total movie time: 62 h 25 min.

Movie S5. Spreading and motion of a cell aggregate on a PAA gel (E = 7.4 kPa) observed in bright field. Total movie time: 39 h 55 min.

Movie S6. Motion of a cell aggregate on a PAA gel (E = 2.8 kPa) observed in bright field. Total movie time: 23 h 50 min.

Movie S7. Motion of a reactive droplet in complete wetting. Total movie time: 338 ms.